PCCP

PAPER

View Article Online
View Journal | View Issue

Cite this: *Phys. Chem. Chem. Phys.*, 2014, **16**, 8392

Electrochemical characteristics of nanostructured platinum electrodes – a cyclic voltammetry study

P. Daubinger,[a] J. Kieninger,*[a] T. Unmüssig[a] and G. A. Urban[ab]

Received 22nd January 2014,
Accepted 17th March 2014

DOI: 10.1039/c4cp00342j

www.rsc.org/pccp

Platinum surfaces play a decisive role in catalysis in sensors, fuel cells, solar cells and other applications like neuronal stimulation and recording. Technical advances in nanotechnology contributed tremendously to the progress in these fields. A fundamental understanding of the chemical and physical interactions between the nanostructured surfaces and electrolytes is essential, but was barely investigated up to now. In this article, we present a wet-chemical process for the deposition of nanostructures on polycrystalline platinum surfaces. The electrochemically active surface area was increased by a factor of over 1000 times with respect to the geometrical surface. The influence of the nanostructures was examined in different acidic, alkaline, and neutral electrolytes. Comparing cyclic voltammograms of nanostructured and planar polycrystalline platinum revealed new insights into the microenvironment at the electrode–electrolyte interface. The characteristic features of the cyclic voltammograms were altered in their shape and strongly shifted with respect to the applied potential. In neutral buffered and unbuffered electrolytes the water window was expanded from 1.4 V to more than 2 V. The shifts were interpreted as local pH-changes and exhausted buffer capacity in direct proximity of the electrode surface due to the strong release and binding of protons, respectively. These polarized electrodes induce significant changes in the electrochemical potential of the electrolyte due to the high roughness of their surface. The electrochemical phenomena and the observed voltage shifts are crucial for the understanding of the basic mechanism at nanostructured electrodes and mandatory for designing fuel cells, sensors and many other devices.

Introduction

Cyclic voltammetry is constantly being used as a powerful and sensitive method to investigate electrode materials.[1] Platinum known for its outstanding catalytic properties[2] and its potential in biomedical engineering[3,4] is therefore applied in many electrochemical applications. Its characteristic cyclic voltammogram (CV) is most likely the best known of all electrode materials. Both planar single crystal and polycrystalline platinum surfaces have been intensively investigated and the processes contributing to the characteristic shape have been well explained. It is known from experiments with single crystal platinum electrodes that the crystal orientations influence the ad- and desorption of reacting species in a CV and therefore cause changes in the peak position and shape of the current density peaks.[5,6]

Platinum structures with high electrochemically active surface areas play a decisive role in efficient catalysis and charge transfer. Advances in these fields were mainly based on progress in nanotechnology. Therefore, platinum nanostructures are of great interest for applications like biosensors,[7–9] biofuel cells,[10,11] alcohol + hydrogen fuel cells,[2,12,13] dye-sensitized solar cells,[14] and neuronal stimulation and recording.[15,16]

In contrast to plane platinum surfaces, the impact of nanostructures on the electrochemical behavior in CVs is not well understood. So far, the influence of the nanostructure in neutral electrolytes has been mainly studied in regard to its current densities[7,17,18] or its charge storage capacity[15] compared to planar electrodes. Whalen *et al.*[19] observed that the electrochemical behavior in phosphate buffered saline (PBS) pH 7.4 significantly alters depending on the nanostructure and morphology of the electrode. However, no explanation of the nanospecific effects was provided.

In order to understand those effects we investigated CVs comparing different electrode morphologies, electrolytes and scan conditions. Comparing neutral pH electrolytes with strongly acidic or alkaline solutions, the characteristic features of the CV are shifted in potential and are changed in its shape. The experimental results lead to a novel explanation of the effects induced by pH changes in the microenvironment at the electrode.

[a] *University of Freiburg, Department of Microsystems Engineering – IMTEK, Laboratory for Sensors, Georges-Koehler-Allee 103, 79110 Freiburg, Germany. E-mail: jochen.kieninger@imtek.uni-freiburg.de; Tel: +49 761 203 7265*
[b] *University of Freiburg, Freiburg Materials Research Center (FMF), Stefan-Meier-Str. 21, 79104 Freiburg, Germany*

Materials and methods

Electrode fabrication and preparation

The polycrystalline platinum electrode chips were fabricated on 100 mm Pyrex borosilicate glass wafers (BOROFLOAT®, SCHOTT AG, Germany) with 500 μm thickness using thin-film technology. Plasma enhanced chemical vapour deposition (PECVD) was used to deposit 200 nm silicon nitride. The metal layers (20 nm titanium, 100 nm platinum, and 50 nm titanium) were formed by physical vapour deposition and structured using a lift-off process. Subsequently, PECVD and reactive ion etching (RIE) were used to deposit and structure the insulation layer consisting of 800 nm silicon nitride and 200 nm silicon oxide. Electrode openings with 200 μm diameter as well as the connecting pads were opened by the RIE step, which also removed the top titanium layer leaving a bare polycrystalline platinum surface. Single electrode chips were obtained by dicing.

In order to obtain clean surfaces and reproducible crystal orientation conditions of the polycrystalline platinum, electrochemical treatment was applied prior to measurements or the deposition of nanostructures. Ten cycles of cyclic voltammograms with a scan rate of 100 mV s^{-1} were conducted in 0.5 M H_2SO_4. Turning points of the CV were chosen to match the onset of hydrogen and oxygen evolution, respectively.

Deposition of nanostructures

Platinum nanostructures were synthesized by colloidal deposition, analogous to the process reported by Sun *et al.*[20] The electrode chips were placed for 7 days in 2 ml of an aqueous solution containing 2.9 mM H_2PtCl_6 (ChemPur Feinchemikalien; Karlsruhe, Germany) and 1.24 M HCOOH (Merck; Darmstadt, Germany). The deposition was followed by the above described electrochemical cleaning step.

Electrochemical measurements

All cyclic voltammograms were repeated multiple times and with separately manufactured electrodes to exclude artefacts in the measurements. The experiments were conducted in acidic, alkaline, and neutral electrolytes: 0.5 M H_2SO_4, 1 M KOH, 0.1 M KCl, 0.1 M NaCl, and 0.1 M phosphate buffered saline (PBS) pH 7.4. PBS consisted of 85.2 mM $Na_2HPO_4{\cdot}12H_2O$, 14.8 mM $NaH_2PO_4{\cdot}H_2O$ and 0.1 M NaCl. Its pH value was adjusted by adding hydrochloric acid (HCl). For measurements with reduced buffer capacity, the 0.1 M PBS solution was diluted with 0.1 M NaCl to 0.01 M solution and afterwards adjusted to pH 7.4 with HCl.

All measurements were controlled using the potentiostat *Autolab PGSTAT126N* and the software *Metrohm NOVA 1.8.* A three-electrode setup was used in all experiments: reference electrode (Ag/AgCl, 3 M KCl; double junction; *Metrohm* 6.07.29.100) using CH_3COOLi as the bridge electrolyte, a counter electrode (*Metrohm* platinum rod, 2 mm in diameter), and the working electrode (200 μm in diameter, see section *Electrode fabrication*). Before each experiment, the electrolyte was degassed with nitrogen gas. During the electrochemical measurements, the electrolyte solution was flushed with nitrogen gas to prevent oxygen from dissolving into the electrolyte. All experiments were performed at room temperature (22 °C ± 1 °C).

The potential scale, which is frequently used in the cyclic voltammograms shown here, is the reversible hydrogen electrode (RHE) scale. The RHE scale compensates the Nernstian influence of the pH value by adjusting the potential (59 mV_{NHE}/pH at T = 298 K).[21,22]

The electrochemically active surface area of the nanowire electrode and therefore the surface roughness Rf were measured by the charge necessary for one monolayer of adsorbed protons.[23,24] These protons are adsorbed and reduced at the electrode surface in a one-electron process:

$$Pt + H^+ + e^- \rightarrow Pt\text{–}H \quad (1)$$

Since the potential turning point in the hydrogen area of CVs influences the Pt–H desorption peaks, it was important to use the Pt–H adsorption peaks in order to characterize the surface roughness. By plotting current density *vs.* time in the CV (Fig. 2), the total charge Q_H is calculated by integrating the current density over time in the region of proton adsorption. The roughness factor Rf is then calculated by dividing the total charge Q_H by the charge density of hydrogen at planar platinum surfaces q_H = 210 μC cm^{-2}.[23]

The nanowire electrodes, which were used throughout the experiments, had a surface roughness factor Rf of around 1000.

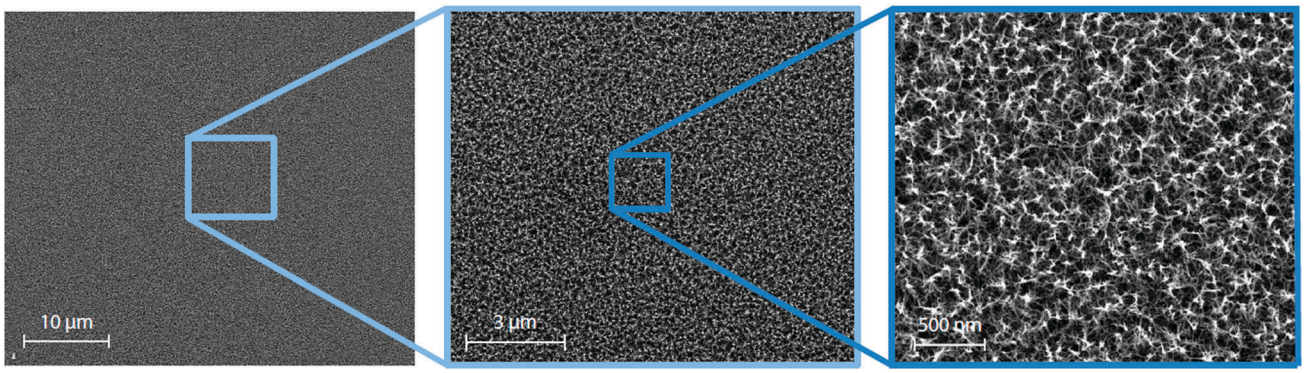

Fig. 1 SEM micrographs of the nanostructured platinum electrode at three different magnifications.

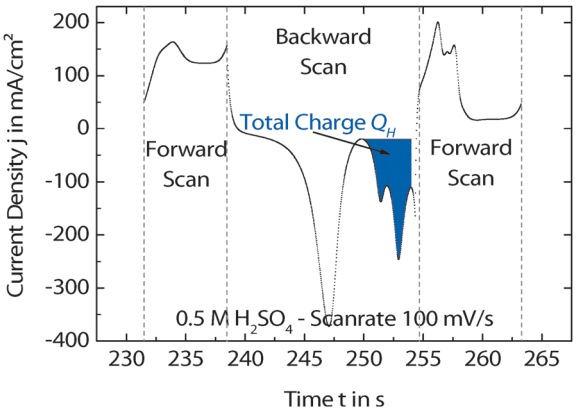

Fig. 2 Graph for determining the electrochemically active surface area of a platinum electrode. The part highlighted in blue shows the area induced by the reduction of adsorbed protons and accordingly the total charge Q_H.

The roughness factors of planar polycrystalline electrodes were approximately 1.

Results and discussion

The morphology of the synthesized platinum nanowires was examined by scanning electron microscopy (SEM; Fig. 1), showing a network of nanowires grown on the electrode surface. SEM investigation of planar polycrystalline electrodes showed a very smooth and homogeneous surface. The results of X-ray photoelectron spectroscopy (not shown here) implied a high purity of the crystalline Pt nanostructures, since no residues resulting from the deposition process were detected. Electrochemical measurements confirmed these facts. Furthermore, new insights into the impact of nanostructured electrodes with high surface roughness on the reactions occurring at the electrode–electrolyte interface were obtained.

Behavior in standard electrolytes

Acidic electrolyte – sulfuric acid (H_2SO_4). The electrochemical response of platinum nanowire electrodes in comparison to planar polycrystalline electrodes in acidic media was investigated using 0.5 M H_2SO_4. A strong increase in current density by three orders of magnitude was observed. Besides, the peak potentials slightly negatively shifted (Fig. 3a; ~ -50 mV). The potential range ΔE (water window) was not significantly affected by the higher surface roughness.

The characteristic shape of the CV with nearly identical peak shapes and positions compared to planar electrodes indicated a polycrystalline nanosurface. Furthermore, the three distinct peaks due to hydrogen desorption indicated a high surface quality. The slightly shifted peak position compared to planar polycrystalline electrodes was assumed to be a surface effect due to different orientations of exposed crystal surfaces. It is unlikely due to pH-shifts or diffusion limitations (see also the next section *Behavior in unbuffered and buffered neutral electrolytes*), since both forward and backward scans were shifted negatively. According to van der Niet *et al.*[6] the crystal orientations influence

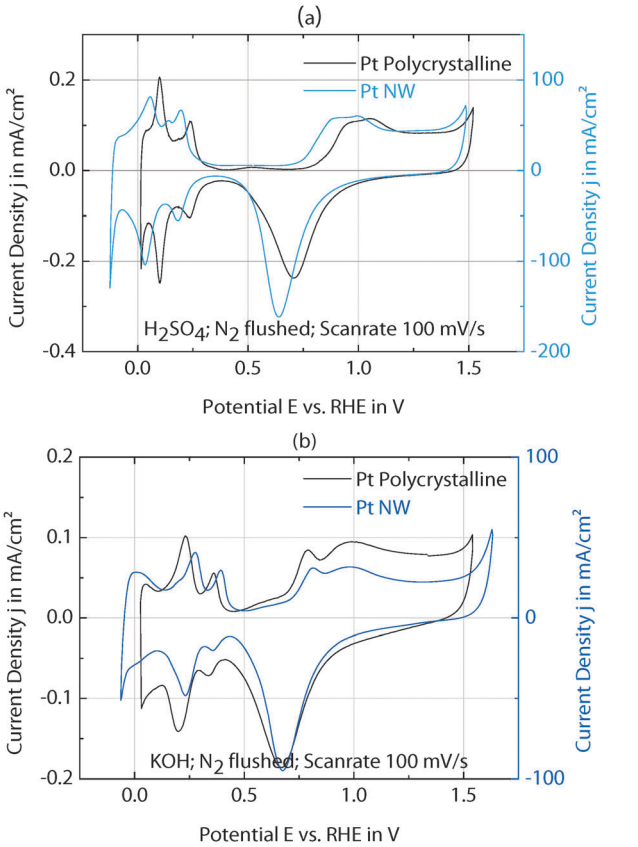

Fig. 3 (a) Comparison of CVs in 0.5 M H_2SO_4: planar polycrystalline and nanostructured platinum electrodes. Please note the different *y*-axis for each graph. (b) Comparison of CVs in 0.1 M KOH: planar polycrystalline and platinum nanowire electrodes. Please note the different *y*-axis for each graph.

the current peak positions, which could possibly explain these small potential shifts.

Alkaline electrolyte – potassium hydroxide (KOH). 1 M KOH was used to investigate the behavior in alkaline media. The increase in current density was analogous to the measurements conducted in sulfuric acid. The water window remained nearly unaffected in both standard electrolytes, when comparing Pt NW electrodes to planar electrodes.

Compared to acidic media, the peak potentials were shifted conversely – in the positive direction (Fig. 3b; $\sim +50$ mV). As previously observed this could be related to a crystal orientation effect that leads to a change in ad- and desorption properties.[6] Strong differences in the electrochemical response were observed in neutral media, which will be discussed in the following section.

Behavior in unbuffered and buffered neutral electrolytes

Unbuffered electrolyte – potassium chloride (KCl). The behavior of nanostructured platinum electrodes in unbuffered neutral media was investigated in a 0.1 M potassium chloride solution (pH $\sim$ 7).

As observed in standard electrolytes, significant increases in current density compared to planar polycrystalline electrodes were measured. While the CV in the case of acidic (alkaline)

media was completely shifted to more negative (positive) regions, the behavior in neutral media is different. Positive voltage shifts of the current peaks were observed in the forward scan and negative shifts in the backward scan. Processes occurring during the forward scan are oxidation reactions along with the release of protons. In contrast, reduction reactions involving the absorption of protons occur during the backward scan. Accordingly, the increased overpotentials indicated a pH-dependent effect. This effect will be described by means of the Pt–H desorption peak. The reaction occurring in this region is described here:

$$\mathrm{Pt{-}H} \rightarrow \mathrm{Pt} + \mathrm{H^+} + \mathrm{e^-} \quad (2)$$

Due to the enlarged electrochemically active surface area, a much higher amount of protons is bound compared to planar polycrystalline electrodes. The acidity influences the electrochemical potential between the electrode and the electrolyte. When protons are released the electrochemical potential of the electrolyte gets increased. Consequently, the strong release of protons led to acidification in direct vicinity of the electrode and a significant increase in overpotential ΔE. In the area of Pt–O formation a similar shift was observed, which can be attributed to the same mechanism.

$$\mathrm{Pt} + \mathrm{H_2O} \rightarrow \mathrm{Pt{-}O} + 2\mathrm{H^+} + 2\mathrm{e^-} \quad (3)$$

In the backward scan, the effect of nanostructured surfaces can be described *vice versa*. Protons, which were involved in both Pt–O reduction and hydrogen adsorption, were depleted in the region close to the electrode. The potential range in which a typical CV is conducted is the range between the evolution of molecular hydrogen and the evolution of molecular oxygen (water window). When this potential range increases, higher overpotentials had to be applied to induce the same reactions. These higher overpotentials lead to expansion of the water window from approx. 1.7 V (polycrystalline electrode) to over 2 V (nanostructured electrode).

Buffered electrolyte – phosphate buffered saline (PBS). Strong differences in the CV characteristics were detected in the neutral electrolyte phosphate buffered saline (PBS). All processes with respect to the applied potential were delayed and expanded over a wider potential range for nanostructured platinum electrodes. Similar to the case of potassium chloride, the water window was expanded from 1.4 V to over 2 V. However, the processes (in the forward scan) started at nearly the same potential as observed for planar polycrystalline electrodes, but with different peak locations.

It was assumed that the buffer system plays a decisive role in the expanded reactions occurring at the nanostructured electrode. Hence, a relationship between these processes and diffusion limitation within the phosphate buffer in direct vicinity of the electrode by the strong release/binding of ions was expected.

Variation of the scan rate. As a consequence of these observations, the scan rate was varied and the CVs were compared to each other. The increase of the scan rate leads to an increase of the current output. In the case of diffusion controlled reactions, the peak current is determined by the Randles–Sevčik equation and is therefore proportional to the square root of the scan rate.[22]

When comparing the transferred charge induced by the adsorption of protons at different scan rates in a linear scan cyclic voltammogram, the same amount of protons was adsorbed at the surface (200 mV s^{-1}: Q_H = 103 mC cm^{-2}; 100 mV s^{-1}: Q_H = 102 mC cm^{-2}, 20 mV s^{-1}: Q_H = 102 mC cm^{-2}). Staircase cyclic voltammetry (SCV), which was used for the slowest scan rate of 2 mV s^{-1} (due to technical reasons), is not suitable for determining the correct charge in time dependent processes like proton adsorption. The differences between SCV and analogous linear scan CV have been investigated by various research groups.[25] Thus the curve with the scan rate of 2 mV s^{-1} can only be treated by its shape, but not quantitatively with respect to the current.

It was observed that in the case of planar electrodes, the water window showed only minor changes. The difference in the water window between the maximum scan rate of 200 mV s^{-1} and the minimum scan rate of 2 mV s^{-1} was around 100 mV. In the case of nanostructured electrodes, the differences were substantially more prominent. By reducing the scan rate, both delay and expansion of the current peaks were decreased. Besides the reduction of overpotentials, the water window strongly decreased with slower scan rates. The difference in the water window between the maximum scan rate of 200 mV s^{-1} and the minimum scan rate of 2 mV s^{-1} was over 600 mV.

Smaller scan rates lead to reduced current densities and a reduced amount of protons, which are bound or released at a given time. In the case of polycrystalline electrodes, the buffer capacity was kept close to the equilibrium state over the whole scan rate range. In contrast, the electrochemical response of nanostructured electrodes was strongly dependent on the scan rate. The expected characteristics of the CV were only obtained with a very slow scan rate of 2 mV s^{-1}. This behavior also indicated diffusion limitation within the phosphate buffer.

It becomes obvious when comparing a slow scan (2 mV s^{-1}) of a nanostructured electrode to a CV of a planar polycrystalline Pt electrode (Fig. 5c). The CV showed the same water window like a polycrystalline electrode. Moreover, the CV was qualitatively nearly identical and the curve showed all the characteristics known for typical planar platinum CVs in PBS. The CV peak positions of nanostructured platinum electrodes converged to the positions of the planar electrodes when the scan rate was reduced (Fig. 6).

Influence of buffer capacity (PBS 100 mM *vs.* 10 mM). In order to get more insights into the role of the buffer, the buffer concentration was reduced from 100 mM (0.1 M NaCl) to a PBS concentration of 10 mM (0.1 M NaCl) with pH 7.4. The results of 10 mM PBS compared to 100 mM PBS (Fig. 7) showed positive shift of the peaks and higher overpotentials in the forward scan. This was not observed for polycrystalline electrodes, where the CV curve progression was similar in both cases (compare Fig. 5c; Pt polycrystalline). In the case of Pt NWs, the processes start at the same potential for both buffer concentrations, but the surface reactions and the peak currents were

significantly expanded on the potential scale for 10 mM PBS (Fig. 7). However, the water window and peak positions in the backward scan remained nearly unchanged.

The difference in the behaviour comparing forward and backward scans is assumed to originate from the nature of the limitation mechanism. In the forward scan the reactions of proton desorption (eqn (2)) and platinum oxide formation (eqn (3)) are independent of the diffusion of protons and thus are limited by the reaction kinetics itself.

On the other hand in the case of the backward scan the reactions for both platinum oxide reduction (reverse reaction of eqn (3)) and hydrogen adsorption (eqn (1)) are dependent on the availability of protons. Thus the reactions are limited by diffusion of protons and buffer components, respectively.

This means that the proton concentration and the pH value in direct vicinity of the electrode were dependent on the scan rate and the reaction kinetics of this process. The buffer capacity was exhausted faster (less current in the beginning) compared to the 100 mM PBS solution, which led to stronger acidification and a positive shift of the Pt–H desorption peak. In the backward scan, protons from the electrolyte solution were involved in the reduction reactions. Consequently, the proton concentration in the electrolyte was the limiting factor for the surface reaction. As the surface reaction with the protons was much faster than the ability of the buffer system to keep its pH constant, the capacity of both buffers was completely exhausted. Accordingly both cyclic voltammograms showed similar behaviour.

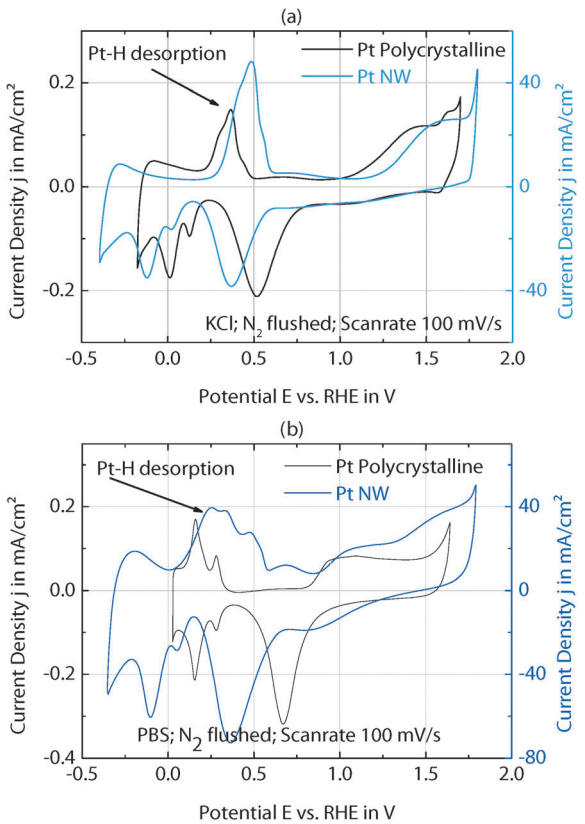

Fig. 4 (a) Comparison of CVs in KCl: polycrystalline and platinum nanowire electrodes. Please note the different *y*-axis for each graph. (b) Comparison of CVs in PBS: polycrystalline and platinum nanowire electrodes. Please note the different *y*-axis for each graph.

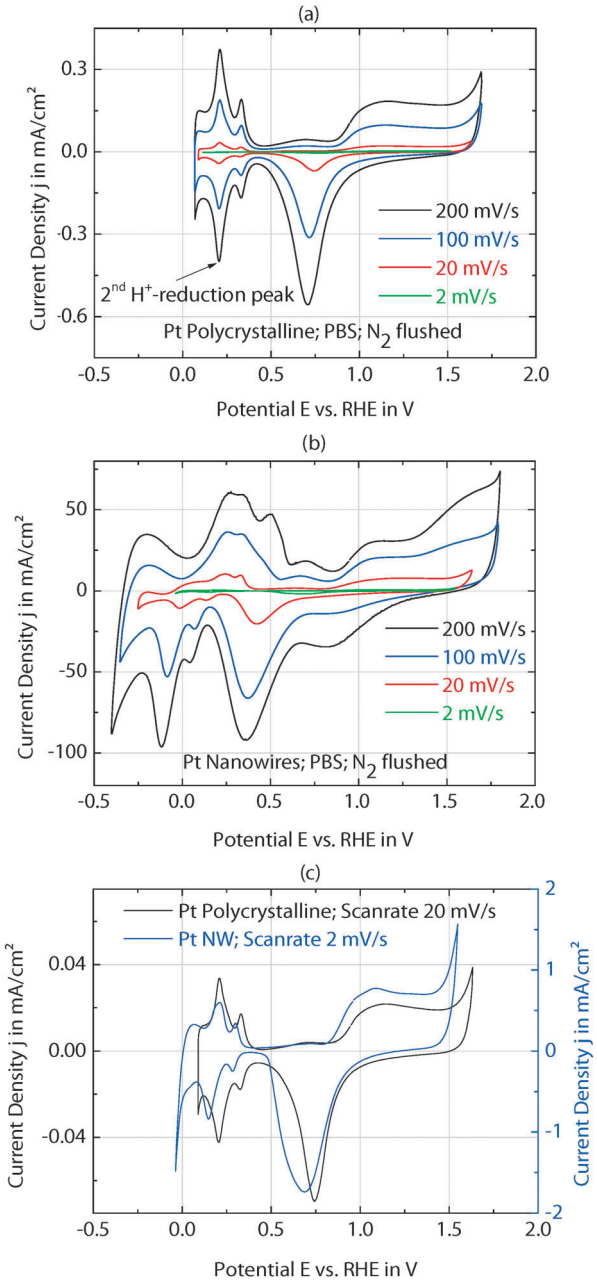

Fig. 5 Comparison of PBS CVs with different scan rates. (a) Shows a planar polycrystalline electrode. (b) Shows the characteristics of a nanostructured electrode. (c) Compares the CV of a nanostructured platinum electrode with a slow scan rate (2 mV s^{-1}) to the CV of a planar polycrystalline electrode.

Another outstanding finding was that the electrochemical response with reduced buffer capacity resembled the characteristics known for CVs of planar polycrystalline platinum electrodes in neutral salt solutions (Fig. 4). This strongly indicated that the shifted Pt–H desorption in neutral salts could be explained by acidification in direct vicinity of the electrode as well.

The reduced buffer capacity of 10 mM PBS only influenced the CVs of nanostructured Pt electrodes, and the CVs of planar

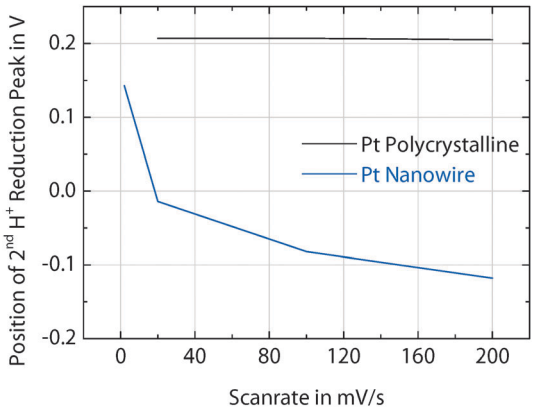

Fig. 6 Current peak positions of the second Pt–H reduction peak (compare Fig. 5a) as a function of the scan rate. The peak positions of polycrystalline Pt electrodes were nearly independent of the scan rate, while in the case of nanostructured Pt electrodes the peaks shifted towards the potential of polycrystalline electrodes when the scan rate was reduced.

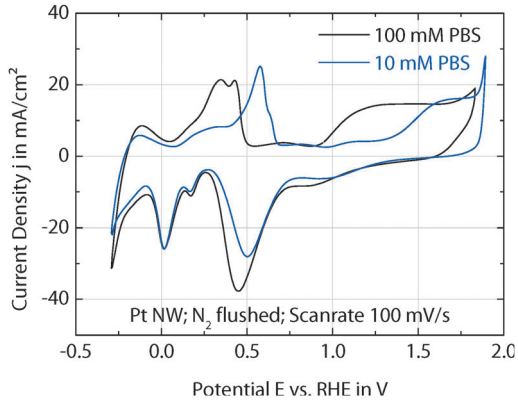

Fig. 7 Comparison of PBS CVs of the Pt NW electrode with different buffer capacity. The black curve shows the CV in standard 100 mM PBS buffer. The blue curve displays the CV with reduced buffer capacity (10 mM PBS). The pH value of 7.4 was similar in both cases.

electrodes remained nearly unchanged compared to 100 mM PBS. However, the CVs of planar Pt electrodes in neutral electrolytes showed a similar effect. The peak was shifted and the water window in KCl was increased to 1.7 V compared to 1.4 V in electrolytes like H_2SO_4, KOH, and PBS.

Cyclic voltammograms in comparison – from pH 0 to pH 14. CVs of planar polycrystalline and nanostructured platinum electrodes in different electrolytes (acidic, alkaline, unbuffered and buffered neutral) were compared to each other. PBS (21 mS cm^{-1}) and KCl (12 mS cm^{-1}) solutions are less conductive than H_2SO_4 (202 mS cm^{-1}) and KOH (190 mS cm^{-1}). However effects due to insufficient conductivity (large iR-drop) would be visible as tilting of the CV curve but not as an increase of the water window.

The comparison showed the influence of the pH value on the current peak positions in a CV and confirmed the presented model of potential shifts due to the high surface area nanoelectrodes.

Throughout this work, all potentials were referenced to the reversible hydrogen electrode (RHE), where the potential was adjusted with a pH correction term (see section *Electrochemical measurements*). In order to estimate the changing pH value in the microenvironment of the electrode–electrolyte interface, the potentials in this section will be referenced to the normal hydrogen electrode (NHE). According to the Nernst equation, the current peak positions of planar polycrystalline Pt electrodes (Fig. 8) were shifted negatively with increasing pH and *vice versa*. The water window of polycrystalline electrodes was similar for sulfuric acid, PBS and potassium hydroxide (each 1.4 V). In the neutral unbuffered electrolyte potassium chloride, the water window was expanded to 1.7 V.

The activity of protons and hydroxide ions, respectively, influences the electrochemical potential of an aqueous electrolyte. At high pH the electrochemical potential of the electrolyte is low and accordingly the processes occur at a lower potential with respect to the NHE. Depending on the pH of the electrolyte, the curves shifted and hence confirmed this fact. The expanded water window for the neutral electrolyte KCl was related to a pH-change in direct vicinity of the electrode, due to acidification (in the forward scan) and alkalization (in the backward scan), respectively. As a result of the high proton/hydroxide ion concentrations in acidic/basic media, this effect did only appear in neutral media.

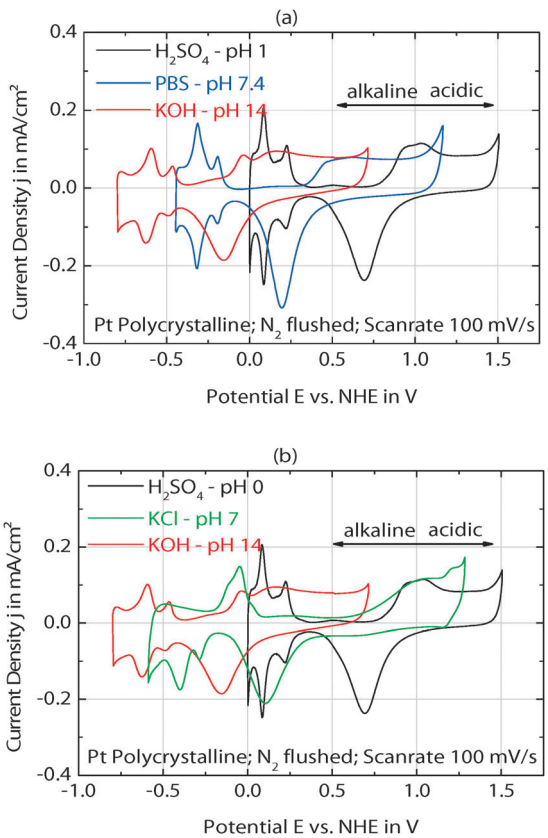

Fig. 8 Comparison of planar polycrystalline platinum CVs in electrolytes with different pH values. The acidity of the electrolyte influences the potential at which the current peaks appear. (a) Shows a comparison between sulfuric acid, phosphate buffered saline (PBS), and potassium hydroxide. In (b) the neutral electrolyte PBS was replaced by potassium chloride. Please note that the potentials were displayed with respect to the normal hydrogen electrode (NHE).

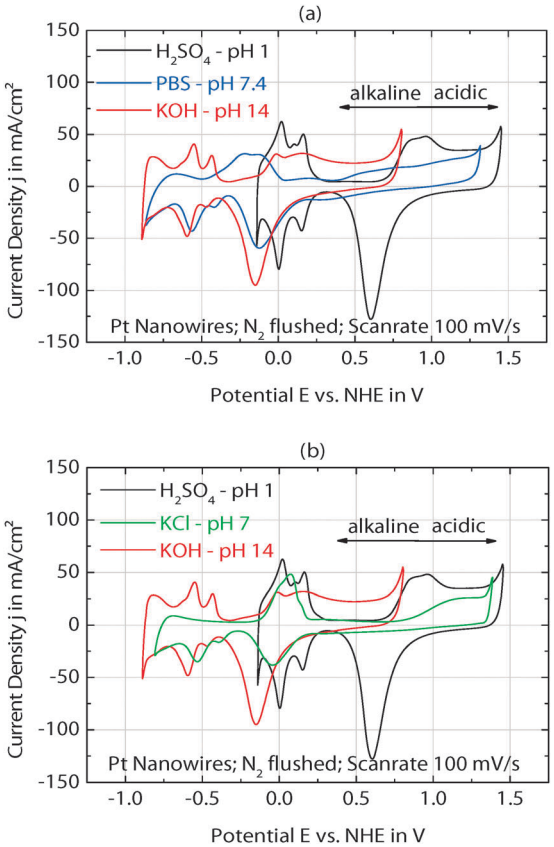

Fig. 9 Comparison of platinum nanowire CVs in electrolytes with different pH values. The left graph shows a comparison between sulfuric acid, potassium chloride, and potassium hydroxide. In the right graph the neutral electrolyte KCl was replaced by phosphate buffered saline. Please note that the potentials were displayed with respect to the normal hydrogen electrode.

The electrochemical response of nanostructured Pt electrodes differed from the results obtained using planar electrodes (see Fig. 9). The water window was similar for sulfuric acid and potassium hydroxide (~1.4 V), but was strongly expanded for both potassium chloride and PBS (~2.0 V). Like in the case of planar polycrystalline Pt electrodes, both water window and potential range remained nearly unchanged for the acidic and the alkaline electrolyte. In contrast, when the measurements were conducted in neutral medium and buffer, much higher overpotentials and an expanded potential range were observed. The features in the forward scan approached the potential region of the acidic medium, and *vice versa* in the regions of the basic medium in the backward scan.

This observation supports the presented model explaining shifts in peak potential depending on local pH changes as a consequence of the high surface area of nanostructured electrodes. The buffer capacity of PBS was not sufficient in the case of nanowire electrodes.

Conclusions

We successfully described the electrochemical phenomena of potential shifts in cyclic voltammograms, which occur at nanostructured platinum electrodes. It was shown that surface reactions on these high surface area electrodes alter the pH-value of neutral electrolytes in direct proximity of the electrode. These shifts of the potential were described by the strong release and binding of protons, respectively. In the forward scan (release of protons) the electrolyte was acidified, and accordingly alkalized in the backward scan. Further, this led to expansion of the potential range (water window) from 1.4 V to 2 V. We assume that these effects are independent of the electrode material used and are only dependent on the electrochemically active surface.

The pH change in the microenvironment at nanostructured Pt electrodes also provided new insights into the CV characteristics known for planar polycrystalline Pt electrodes in neutral salt solutions like potassium and sodium chloride. The CVs of those neutral electrolytes show effects analogous to those of nanostructured electrodes, but are less prominent.

Experiments conducted in phosphate buffered saline (PBS) showed a change in the shape of CVs of nanostructured platinum electrodes compared to polycrystalline electrodes, in addition to the phenomena described above. Besides potential shifts and increase of the water window, the exhausted buffer capacity induced the expansion and flattening of typical features.

We assume that the presented model of potential shifts is universally observed at nanostructured electrodes. The understanding of the basic relationship between the electrochemically active surface area and its influence on the potential is critical for the design of nanostructured electrochemical devices.

Acknowledgements

Financial support: Project no. HEALTH-F2-2009-222741, acronym "METOXIA", in the 7th Framework Program of the European Union.

Notes and references

1 J. Heinze, *Angew. Chem., Int. Ed. Engl.*, 1984, **23**, 831–981.
2 M. K. Debe, *Nature*, 2012, **486**, 43–51.
3 A. Cowley and B. Woodward, *Platinum Met. Rev.*, 2011, **55**, 98–107.
4 J. Gopal, N. Hasan, M. Manikandan and H.-F. Wu, *Sci. Rep.*, 2013, **3**(1260), 1–8.
5 J. Clavilier, K. El Achi and A. Rodes, *Chem. Phys.*, 1990, **141**, 1–14.
6 M. J. van der Niet, N. Garcia-Araez, J. Hernández, J. M. Feliu and M. T. Koper, *Catal. Today*, 2013, **202**, 105–113.
7 D. Wang, R. Kou, M. P. Gil, H. P. Jakobson, J. Tang, D. Yu and Y. Lu, *J. Nanosci. Nanotechnol.*, 2005, **5**, 1904–1909.
8 C. H. Chou, J. C. Chen, C. C. Tai, I. Sun and J. M. Zen, *Electroanalysis*, 2008, **20**, 771–775.
9 J. Wang, *Chem. Rev.*, 2008, **108**, 814–825.
10 A. Kloke, C. Köhler, R. Gerwig, R. Zengerle and S. Kerzenmacher, *Adv. Mater.*, 2012, **160**, 2916–2921.
11 S. Cosnier, A. Le Goff and M. Holzinger, *Electrochem. Commun.*, 2014, **38**, 19–23.

12 V. Rao, C. Cremers, U. Stimming, L. Cao, S. Sun and S. Yan, *J. Electrochem. Soc.*, 2007, **154**, B1138–B1147.
13 A. Kowal, M. Li, M. Shao, K. Sasaki, M. B. Vukmirovic and J. Zhang, *Nat. Mater.*, 2009, **8**, 325–330.
14 T. L. Hsieh, H. W. Chen, C. W. Kung, C. C. Wang, R. Vittal and K. C. Ho, *J. Mater. Chem.*, 2012, **22**, 5550–5559.
15 S. F. Cogan, *Annu. Rev. Biomed. Eng.*, 2008, **10**, 275–309.
16 Y. H. Jin, P. Daubinger, B. Fiebich, T. Stieglitz, *MEMS IEEE 24th International Conference*, 2011, 1003–1006.
17 C. Luhana, X. J. Bo, J. Ju and L. P. Guo, *J. Nanopart. Res.*, 2012, **14**, 1158.
18 J. H. Yuan, K. Wang and X. H. Xia, *Adv. Funct. Mater.*, 2005, **15**, 803–809.
19 J. J. Whalen, J. Young, J. D. Weiland and P. C. Searson, *J. Electrochem. Soc.*, 2006, **153**, C834–C839.
20 S. Sun, F. Jaouen and J. P. Dodelet, *Adv. Mater.*, 2008, **20**, 3900–3904.
21 G. G. Libowitz and M. S. Whittingham, *Materials Science in Energy Technology*, Academic Press, 1979.
22 C. G. Zoski, *Handbook of Electrochemistry*, Elsevier publications, 2007.
23 T. Biegler, D. A. Rand and R. J. Woods, *J. Electroanal. Chem.*, 1971, **29**, 269–277.
24 J. M. Rodríguez, J. Melián, J. A. Herrera and J. P. Peña, *J. Chem. Educ.*, 2000, **77**, 1195–1197.
25 B. Hai, Y. V. Tolmachev, K. A. Loparo, C. Zanelli and D. Scherson, *J. Electrochem. Soc.*, 2011, **158**, F15.